# Co-simulation studies of optimal control for natural refrigerant heat pumps

*Thibault* Péan [a], *Daniel Ramón* Lumbieres [a], *Alba* Colet [a], *Ivan* Bellanco [a], *Martin Josef* Neugebauer [b], *Daniel* Carbonell [b], *Jon* Iturralde Iñarga [c], *Cristina* Corchero García [a,d], *Jaume* Salom [a]

[a] Catalonia Institute for Energy Research (IREC), Sant Adrià de Besòs (Barcelona), Spain, tpean@irec.cat.

[b] SPF-OST Institut für Solartechnik, Rapperswil, Switzerland.

[c] Fundación Tecnalia Research and Innovation, Azpeitia (Gipuzkoa), Spain.

[d] Universitat Politècnica de Catalunya (UPC), Barcelona, Spain.

**Abstract.** The object of the present study is a natural refrigerant base (propane) heat pump system with a dual source/dual sink heat exchanger (air or ground-based) which is integrated into a centralized tri-generation system with PV and battery for a multi-family building located in Spain. To evaluate the performance of this complex system, a simulation environment was developed, connecting different software. The main program is TRNSYS, with the python package pytrnsys used to create the models and run the simulations, while a model predictive controller is externalized in a separate optimization software. The co-simulation environment enables to couple both software and operate the models in the simulation with the decisions made by the external controller. This environment was used to evaluate the considered system for three separate weeks of the year, each representative of the heating/cooling/DHW demands in winter, summer and intermediate seasons. For each of these weeks, the simulation was run once with a reference rule-based controller, and once with the advanced model predictive controller, to evaluate the additional benefits brought by the later strategy. The results were then extrapolated to the whole year, and revealed that the model predictive controller was able to provide cost savings of 12 to 20% (depending on the consideration or not of the cooling season which gave unexpectedly adverse results). This controller operated the heat pump more efficiently thanks to its prior knowledge of the best source to use at each moment (air or ground). It also managed the battery in a more economical way thanks to its prior knowledge of the time-varying electricity price, thus charging always at the cheaper hours of the day, and demonstrating the advantages of using forecasts and predictive optimization for HVAC control.

**Keywords.** Heat pumps, co-simulation, model predictive control, tri-generation systems
**DOI:** https://doi.org/10.34641/clima.2022.432

## 1. Introduction

Heat pumps have an important role in the decarbonisation of the building sector, thanks to their high efficiency and the possibility to operate them with renewable electricity. The corresponding market has been growing rapidly in the last years, with an increase from 893 k units sold in Europe in 2015 to 1.6 m in 2020 [1]. Furthermore, the Kigali amendment to the Montreal Protocol [2] will enforce a limit on the global warming potential of the refrigerants used in heat pumping systems, which will drive a shift towards natural refrigerants or less environmentally damaging substances.

Centralized heat pump installations for multi-family buildings present several advantages, including the economy of scale for the buffer storages in common spaces of the building. In this paper, a dual source/sink heat pump system adapted to mild Mediterranean climates is investigated. This heat pump includes a dual source heat exchanger that is able to transfer heat with either a geothermal or an air source/sink, and which can work as evaporator or condenser in heating or cooling modes respectively. Both sides can be switched depending on which is the most efficient heat source or sink at any moment. Such a system enables to downsize the length of the costly borehole by a factor of two, since part of the yearly load can be covered with the air source. Furthermore, the dual source/sink heat pump uses propane (R290) as a refrigerant, which has a much lower global warming potential than most refrigerants currently used in thermodynamic cycles, and therefore presents less potential impacts

in case of leakages.

To fully exploit the cost and carbon emission savings potential of heat pump systems, they must be controlled and operated in a smart manner. In this regard, model predictive controls (MPC) based on optimization and predictions of the future have proven to be a promising solution. It has been demonstrated that such strategies can provide savings of up to 30% in several cases [3].

The present study evaluates the benefits of the centralized dual source/sink system for a multi-family building. Through detailed simulations performed in co-simulation between different software, the complete studied system was evaluated under two different strategies: a reference rule-based control, and an advanced controller based on model predictive control. Selected representative weeks were chosen to perform these detailed simulations.

## 2. Methodology

The dynamic simulations performed for this study have been carried out in a software environment involving different interconnected programs. This simulation environment is first presented, then the study case is described with details of all the systems considered, and their control strategies. Finally, the weeks chosen for the analysis are presented.

### *2.1. Simulation environment*

The simulation environment is based on the pytrnsys package [4], which is a complete framework to create, run and post-process TRNSYS simulation models in python. All the systems are represented with detailed models connected together with the pytrnsys interface. In the present case, two different control strategies have been used: a reference control, which was integrated directly in the TRNSYS models, and an advanced energy management (AEM) which is based on optimization and therefore has to be externalized.

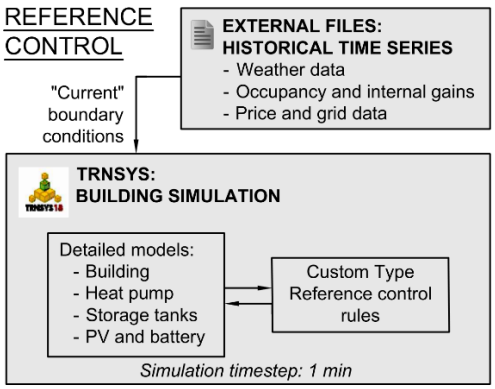


**Fig. 1 –** Architecture of the simulation environment in the reference control case.

The reference control schematic is presented in Fig. 1. In that case, the rules composing the reference control are implemented into a custom TRNSYS Type that manages the operation of the different systems.

The advanced control schematic is presented in Fig. 2. In that case, the controller (AEM) is written in an external GAMS code [5]. The simulation has a time step of 1 minute, and every 15 minutes, the AEM controller is called: first, a communication is established between a python script and TRNSYS (Type163) through read/write files. Afterwards the python script launches the GAMS model which performs its optimization calculations and returns its output to TRNSYS through python. In this way, the AEMS determines the optimal set-points for the next 15 minutes of simulation, which are then interpreted in TRNSYS by a custom Type and applied to the models of the different systems. This process is repeated after 15 minutes.

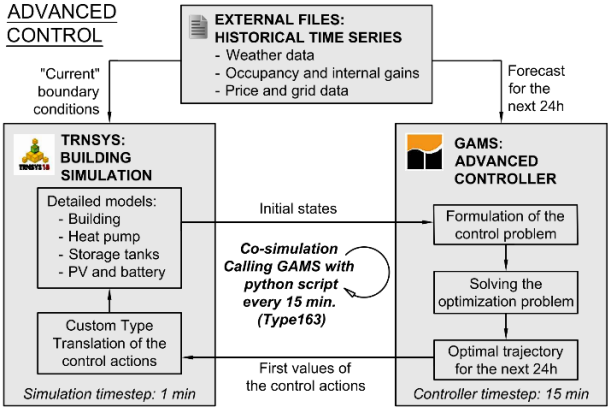


**Fig. 2 –** Architecture of the simulation environment in the advanced control case.

### *2.2. Characteristics of the study case*

The study case presented in this paper is a multi-family building situated in Tarragona, Spain, with a total heated surface area of 2400 m$^2$. The heating and cooling systems are centralized and distribute the required power to the 38 flats that comprise the building.

The centralized systems consist of:

- A dual source/sink reversible heat pump with a dual source/sink heat exchanger (DSHX), capable of using either air or ground as sources (DSHX as evaporator) and sinks (DSHX as condenser).
- Two storage tanks, one for storing domestic hot water (DHW) and one for space conditioning including both space heating (SH) and cooling (SC).
- An electrical system composed of a photovoltaic field (PV) and an electrical battery that enables to store the surplus of electricity not directly consumed in the building.

Space heating is distributed to the flats through distribution pipes and a radiant floor system. Space cooling is distributed using fan coil units (FCU). The

DHW distribution system includes a recirculation loop to keep the piping to each apartment warm.
A conceptual schematic of the mechanical and electrical systems is presented in Fig. 3 and the list of subsystems and their respective sizes in the considered study case is presented in Tab. 1.

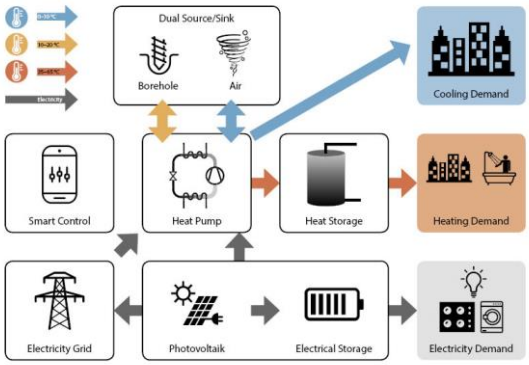


**Fig. 3** – Conceptual view of the overall mechanical and electrical systems.

**Tab. 1 –** List and sizes of the considered systems for the study case of Tarragona.

| Parameter | Unit | Value |
|---|---|---|
| Heat pump power | kW | 44 |
| DHW tank capacity | $m^3$ | 1.75 |
| SH/SC tank capacity | $m^3$ | 1.5 |
| PV peak power | kWp | 62.5 |
| Battery capacity | kWh | 125 |
| Heating demand | $kWh/m^2$ | 2.0 |
| Cooling demand | $kWh/m^2$ | 7.0 |
| Appliances elec. demand | $kWh/m^2$ | 31.5 |

### *2.3. Control strategies*

The reference control for the dual source system consists in a set of rules that decide on the operation of its different components. The algorithm is split between heating and cooling modes. The temperatures in the two tanks and their associated set-points determine whether there is a demand for space heating, cooling or DHW. The demand is mainly covered by the heat pump with priority on DHW. The algorithm determines which is the most efficient source or sink (air or ground) for the DSHX at each moment, i.e. the warmest source is considered the most efficient in heating mode, while it is the coolest in heating mode. When both sources/sinks have the same temperature, the ground source is favoured. The room temperature demand is determined by a classic thermostatic control. In addition, in cooling mode, a free cooling operation is possible and prioritized: it consists in circulating water between the radiant floor circuit and the borehole to cool down the building. If this is not sufficient, cold water from the space conditioning tank is provided to the FCU to further cool down the rooms.

The advanced control presents a different approach based on model predictive control. It consists of an optimization problem that minimizes operational costs and discomfort. The optimization module uses reduced-order models of the system that enables it to project its operation into the future. It is also fed with weather forecasts, occupancy and energy prices. The optimization problem is solved every 15 minutes and sends the required set-points to the "real" (simulated) system, to which the set-points are applied in the TRNSYS simulation. The main configurational parameters of the model predictive control are presented in Tab. 2. The thermal systems are represented as RC models, as shown in Fig. 4. The heat pump is represented by a linear model which expresses its electrical consumption in function of the ambient temperature, the supply temperature and the thermal power delivered [6].

**Tab. 2 –** Configurational parameters of the model predictive controller.

| | |
|---|---|
| Building model | R2C2 |
| Tanks model | R1C1 |
| HP model | Linear |
| Horizon length | 24h |
| Time step | 15 min |
| Optimization criteria | 5% relative gap |

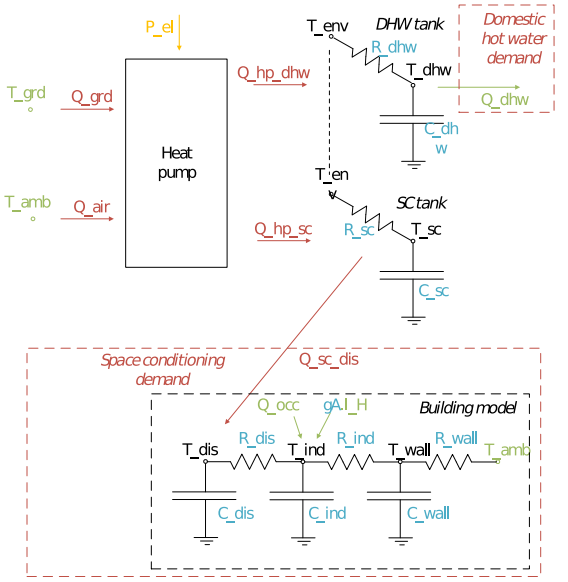


**Fig. 4** – Simplified models of the considered systems (thermal part).

### *2.4. Simulated weeks*

Three different weeks of the year have been simulated, covering the specific seasons encountered in the climate of Tarragona, Spain. These specific weeks were chosen as representative of their respective season, enabling an extrapolation to the whole year. The methodology for selecting the representative weeks followed these two main steps:

- Grouping all the weeks of the year into 4 different clusters using their average outdoor temperature and summed solar irradiation (using a k-means algorithm) [7],

- Within each cluster, choosing the week that is most representative of the cluster according to its space heating or cooling load (using a genetic algorithm) [7]

Following this process, one week was selected for the heating dominated cluster (January 18th to 24th) and one week for the cooling dominated cluster (July 4th to 10th). For the two remaining intermediate clusters with little to no space conditioning load, only one week was selected to represent both of them (April 10th to 16th), since they only have DHW load.

The weather conditions of the three selected weeks are represented in Fig. 5, with both the outdoor ambient temperature and the horizontal solar irradiation. In addition, the price signal for the first week has been plotted. This price signal represents one typical week, with high prices between 10:00 – 14:00 h and between 18:00 – 22:00 h in weekdays, while the weekends see low prices all day long. Here, the Saturday and Sunday are in the middle of the chosen 7 days (Jan. 20th and 21st). The price signal is the same for the other weeks, therefore they are not presented again, although the Saturday and Sunday fall to different positions.

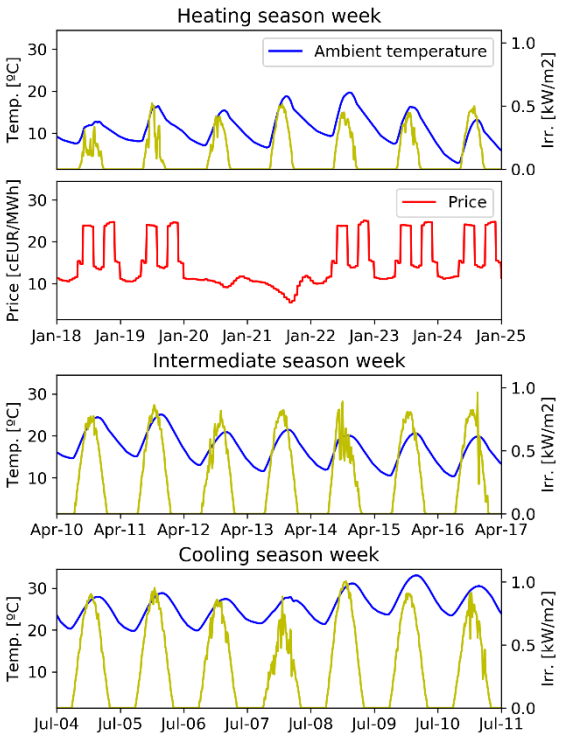


**Fig. 5 –** Representation of the three selected weeks.

Another important hypothesis is the impossibility to sell the excess electricity produced by the PV panels to the grid. Although the export is possible, it is not rewarded economically.

Regarding the interpretation of the results, several Key Performance Indicators (KPIs) have been calculated, among which the amount of electricity imported from the grid, the electricity from the PV that is exported to the grid, the average COP (averaged for COP and EER when operating for both DHW and SC in the cooling season), and the thermal energy produced by the heat pump for each use. Other KPIs are described in [8].

# 3. Results

## *3.1. Heating season week (winter)*

The results are first analysed for the winter week in the heating season, which ranges from the 18th to the 24th of January. Fig. 6 presents the electricity imported from the grid in both the reference and the advanced control cases as well as the resulting energy cost. The periods of high prices have been represented in light red to highlight the moments of high penalty where the import of energy should be avoided.

**Tab. 3 –** Main KPIs computed for the reference and advanced control cases of the winter week, and the difference between both cases [8].

| Parameter | Ref. | AEMS | Diff. (%) |
|---|---|---|---|
| Cost of imported electricity [EUR] | 85.1 | 69.6 | -15.5 (-18.2%) |
| Electricity import from grid [kWh] | 646.9 | 670.8 | +24.0 (+3.7%) |
| Electricity export to grid [kWh] | 0 | 3.28 | +3.27 |
| Average COP [-] | 3.23 | 3.50 | +0.26 (+8%) |
| Thermal energy produced SH [kWh] | 300.4 | 245.5 | -54.9 (-18.3%) |
| Thermal energy produced DHW [kWh] | 859.3 | 914.1 | 54.9 (+6.40%) |
| Comfort time in Cat. I [%] | 83.2% | 46.5% | -36.7% |
| Comfort time in Cat. II [%] | 16.8% | 53.5% | +36.7% |
| Average room temperature [ºC] | 21.2 | 21.0 | -0.23 |
| Grid purchase ratio [%] | 0.36 | 0.37 | +0.02 |
| PV generation ratio [%] | 0.68 | 0.69 | +0.01 |
| Renewable primary energy [kWh] | 2299 | 2321 | +21.8 (+1.0%) |
| Total primary energy [kWh] | 3563 | 3631 | +68.7 (+1.90%) |
| Renewable Energy Ratio [%] | 0.65 | 0.64 | -0.01 |

It can first be observed that the reference control strategy actually performs well with regards to avoiding these high cost periods. In the hours of solar irradiation in the middle of the day, it charges the battery, and when the sun sets, it can use the charged energy: this moment coincides with the high price period of the night, and therefore the import of electricity is generally avoided at these times. The advanced control goes one step further by optimizing

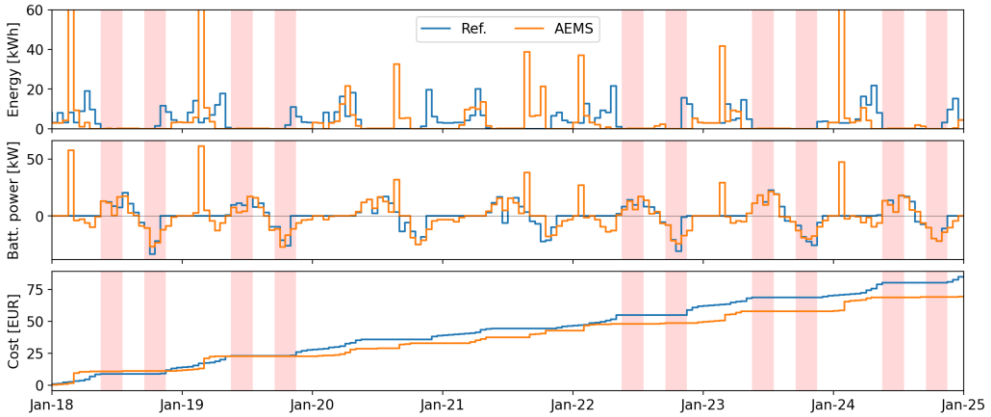


**Fig. 6 –** Hourly electricity import, battery power and cumulative energy cost compared for both the reference and advanced control cases in the winter week. Red shaded represents periods of high electricity prices.

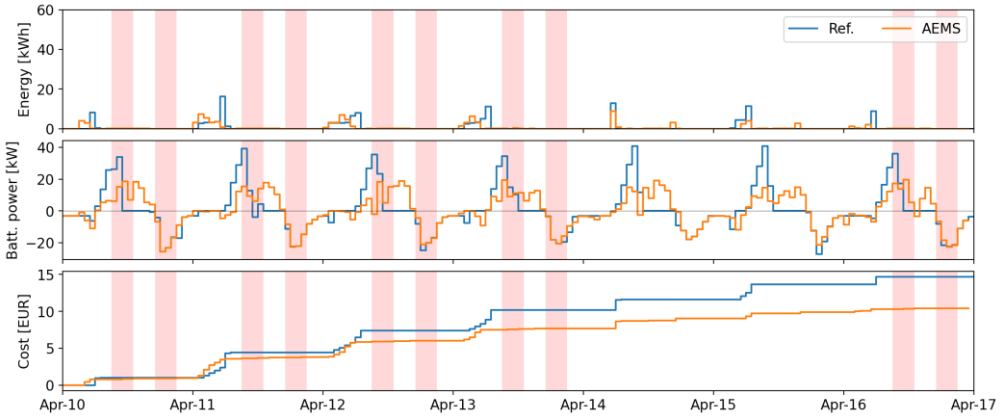


**Fig. 7** – Hourly electricity import, battery power and cumulative energy cost compared for both the reference and advanced control cases in the intermediate week. Red shaded represents periods of high electricity prices.

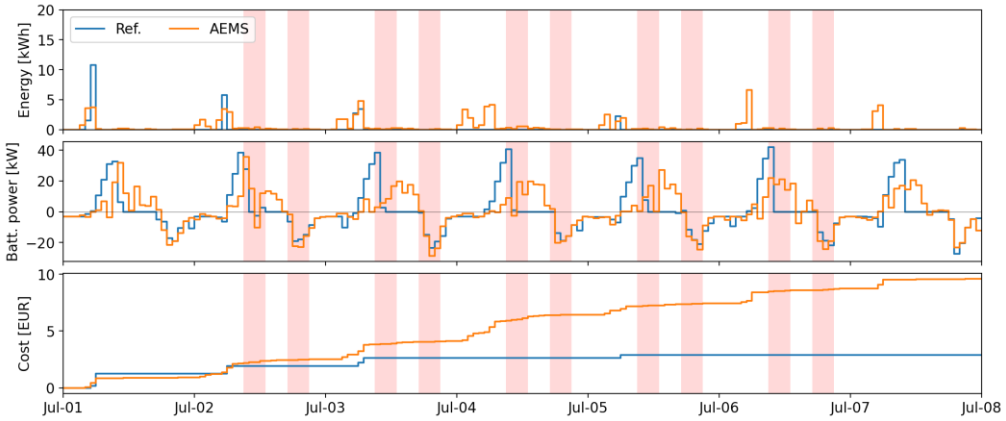


**Fig. 8** – Hourly electricity import, battery power and cumulative energy cost compared for both the reference and advanced control cases in the summer week. Red shaded represents periods of high electricity prices.

the charging of the battery considering the energy price. A peak of energy import from the grid can be observed during certain nights: during this hour, the price is minimal over the rolling 24 hour horizon, therefore the advanced controller makes the most of it by fully charging the battery with the energy that will not anyways be available with solar power on the next day.

This operation enables to provide additional cost savings which is the final objective of the implemented control, as can be seen in Tab. 3 where the main KPIs that have been computed are presented. Although the amount of electricity imported from the grid slightly increases (+3.7%) due to this night charging operation, the energy operational costs decrease by 18%. It should be noted that the dual source heat pump operates at a higher efficiency with the advanced controller, since it knows the temperature evolution of both sources

and the resulting COP of the heat pump in those conditions in advance. The average COP for that week therefore increases from 3.23 to 3.50. Thermal comfort slightly decreases: the average room temperature is 21.2 °C in the reference case, while it is reduced to 21.0 °C with the advanced control. This slight difference is not considered to affect the occupants since thermal comfort always stays within the comfort categories I or II from the European standards on Indoor Environmental Quality [9].

### *3.2. Intermediate season week (spring)*

The results of the intermediate season week are analysed next. For this case, it is a week with a mild climate which does not require active heating or cooling, and where thermal comfort can be achieved with passive strategies such as natural ventilation. The main thermal load is therefore DHW in this scenario. The imported electricity and cumulative cost in both control strategies are reported in Fig. 7.

In this scenario, both control strategies avoid the highest price periods to import electricity. However, the import peaks always happen at the lowest price hour for the advanced control, and a few hours later for the reference rule-based control. The main computed KPIs are presented in Tab. 4. The cost savings are lower in absolute values than in the heating case since the demand is also lower. However, in relative savings, the advanced control manages to reduce the electricity import from the grid by 28.5%, which then corresponds to cost savings of 29%, this despite a slight increase of the thermal energy produced for DHW (+5.5%). The heat pump is also operated at higher efficiency since the average COP increases from 3.44 to 3.96 thanks to the advanced control.

**Tab. 4** – Main KPIs computed for the reference and advanced control cases of the intermediate week, and the difference between both cases.

| Parameter | Ref. | AEMS | Diff (%) |
|---|---|---|---|
| Cost of imported electricity [EUR] | 14.7 | 10.4 | -4.3 (-29.0%) |
| Electricity import from grid [kWh] | 132.1 | 94.5 | -37.6 (-28.5%) |
| Electricity export to grid [kWh] | 985.8 | 962.8 | -23.0 (-2.3%) |
| Average COP [-] | 3.44 | 3.94 | +0.50 |
| Thermal energy produced SH [kWh] | 0.0 | 0.0 | 0.0 |
| Thermal energy produced DHW [kWh] | 747.9 | 788.9 | +41.0 (+5.5%) |
| Grid purchase ratio [%] | 0.08 | 0.06 | -0.02 |
| PV generation ratio [%] | 1.59 | 1.61 | +0.02 |
| Renewable primary energy [kWh] | 2198 | 2287 | +88 (+4.0%) |
| Total primary energy [kWh] | 2456 | 2471 | +15 (+0.6%) |
| Renewable Energy Ratio [%] | 0.89 | 0.93 | +0.03 |

### *3.3. Cooling season week (summer)*

Finally, we analyse the results of the week of the cooling season. In that case, the building can be cooled down using the borehole in a free cooling operation, or with active cooling using the cold water produced by the heat pump and stored in the space conditioning tank.

It should be noted that the cooling case with the advanced controller does not perform as expected. This is notably due to the higher complexity of the optimization problem with the additional free cooling variables, and the differences in the model parameters. For these reasons, the optimization fails to converge and to provide a solution within its allocated time (300 seconds for each optimization) for a significant number of instances. When such error occurs, the set-points are not updated, and thus it disturbs the strategy that had been planned until that moment, since local changes must be adapted to continue operating the systems.

**Tab. 5 –** Main KPIs computed for the reference and advanced control cases of the summer week, and the difference between both cases.

| Parameter | Ref. | AEMS | Diff (%) |
|---|---|---|---|
| Cost of imported electricity [EUR] | 2.89 | 9.59 | +6.7 (+232%) |
| Electricity import from grid [kWh] | 26.5 | 79.1 | +52.6 (+198%) |
| Electricity export to grid [kWh] | 1522 | 916 | -606 (-40%) |
| Average COP [-] | 3.82 | 3.86 | +0.05 (+1.2%) |
| Thermal energy produced SC [kWh] | 21.1 | 2318 | +2297 |
| Thermal energy produced DHW [kWh] | 685 | 731 | +46 (+6.8%) |
| Free cooling energy [kWh] | 1980 | 568 | -1411 (-71%) |
| Comfort time in Cat. I [%] | 100% | 100% | - |
| Average room temperature [ºC] | 24.1 | 23.6 | -0.48 |
| Grid purchase ratio [%] | 0.02 | 0.03 | +0.02 |
| PV generation ratio [%] | 2.02 | 1.43 | -0.59 |
| Renewable primary energy [kWh] | 2281 | 2325 | +44 (+1.9%) |
| Total primary energy [kWh] | 2333 | 2480 | +147 (+6.3%) |
| Renewable Energy Ratio [%] | 0.98 | 0.94 | -0.04 |

The KPIs are presented in Tab. 5 and the time series (import, battery and cumulative cost) in Fig. 5. These results should be considered with caution because of the aforementioned faulty operation. In this considered summer week, the PV production is high and should suffice to cover almost all the electrical load of the building. The imported electricity is therefore small in both cases (26.5 and 79.1 kWh), although the advanced controller case actually imports more energy than the reference controller

case.

It can also be observed that the advanced controller performs worse than the reference one when it comes to the choice of the cooling strategy. Most of the cooling load is covered by free cooling with the reference controller, a strategy that has little to no cost (only circulation pumping). The advanced controller on the other hand resorts a lot to active cooling with the heat pump and the FCU. We suspect that the simplified model for the ground temperature used in the AEMS, which has large effects on the free cooling operation, is the main cause of such discrepancies and we are trying to solve this issue.

### *3.4. Yearly results extrapolation*

The results of the separate weeks for each season have been presented in the previous section. An annual interpretation can then be carried out, by considering that the chosen weeks are representative of their respective seasons, and that the other weeks of their cluster will present similar levels of energy costs. The energy cost for each of the studied week and the extrapolation is reported in Tab. 6. Given the number of weeks in each cluster, the total cost for each season can be computed, which then gives the sum of the annual energy costs. In that case, the reference control would result in an annual cost of 1889 € against 1651 € for the advanced controller, hence the AEMS provides cost savings of 12.6%.

Given the uncertainty of the cooling week results, a separate sum considering only the heating and intermediate seasons has also been computed. In that case, the adverse effects of the cooling week performance are less notable, and therefore the cost savings reach a value close to 20% which complies with the 15% objective that had been envisioned for this type of system operated with the advanced controller.

**Tab. 6** – Interpretation of yearly results.

| | **Number of weeks [-]** | **Cost Ref. week [EUR]** | **Cost AEMS week [EUR]** | **Season cost Ref. [EUR]** | **Season cost AEMS [EUR]** | **Savings [%]** |
|---|---|---|---|---|---|---|
| Heating season | 19 | 85.1 | 69.6 | 1616.9 | 1322.4 | |
| Intermediate season | 15 | 14.7 | 10.4 | 220.5 | 156 | |
| Cooling season | 18 | 2.89 | 9.59 | 52.0 | 172.6 | |
| Yearly total | 52 | | | 1889.4 | 1651.0 | -12.6% |
| Yearly total (without cooling) | 34 | | | 1837.4 | 1478.4 | -19.5% |

## 4. Conclusions

The study has first presented an innovative simulation framework including different interconnected software. This platform enables the testing of different controllers in an automated way, particularly of advanced controllers based on optimization which cannot be included in the main simulation software and must be externalized. It was shown that the communication between the different pieces of software functions correctly and that the overall simulation framework performs satisfactorily. This developed environment is an important outcome of the study that can be reused for further research.

In that simulation environment, a dual source/dual sink system adapted to a Mediterranean climate has been tested for three separate representative weeks. The overall HVAC system performs satisfactorily with a reference controller, but the advanced controller based on model predictive control enables to save an additional 12% to 19% on the energy costs annually. The advanced controller manages the heat pump in a more efficient way, benefitting from its knowledge in advance of the most efficient of the two available sources (air or ground) at every moment. The battery is also managed more efficiently according to the considered price signal, with charging hours coinciding with the lowest electricity prices.

As further research, the optimization problem of the advanced controller in cooling mode should be revised to obtain faster and more reliable results. Furthermore, a second system which includes additional elements will also be tested. This new system comprises a solar thermal collector and an ice slurry storage, hence the advanced controller will additionally manage these elements to optimize the operation of the whole system. This other system is a study case in another climate (Switzerland), thus enabling to have a better overview of the controller performance in a variety of climates and conditions.

## 5. Acknowledgement

The research conducted in this paper is funded by the European Union Horizon 2020 Research and Innovation program under grant agreement no. 814888 (TRI-HP).

## 6. References

[1] European Heat Pump Association. EHPA stats 2021. http://stats.ehpa.org

(accessed August 18, 2021).
[2] UN. Amendment to the Montreal Protocol on Substances that Deplete the Ozone Layer. Kigali: 2016.
[3] Péan T, Salom J, Costa-Castelló R. Review of control strategies for improving the energy flexibility provided by heat pump systems in buildings. J Process Control 2018;74:35–49. https://doi.org/10.1016/j.jprocont.2018.03.006.
[4] SPF-OST. pytrnsys 2021. https://pytrnsys.readthedocs.io/en/latest/.
[5] GAMS Development Corp. General Algebraic Modeling System (GAMS) 2021.
[6] Péan T. Heat pump controls to exploit the energy flexibility of building thermal loads. Universitat Politècnica de Catalunya, 2020.
[7] Haberl R, Schubert M, Péan T, Bellanco I, Belio F, Salom J. TRI-HP D7.1 - Concise Cycle Test (CCT) method definition. Rapperswil, Switzerland: 2021.
[8] Iturralde J, Alonso L, Pascual C, Hernandez P. TRI-HP D1.2 - Technical, economic and environmental performance KPIs definition. 2020.
[9] Mendoza-Serrano DI, Chmielewski DJ, Ieee. Controller and System Design for HVAC with Thermal Energy Storage. 2012 Am Control Conf 2012:3669–74. https://doi.org/10.1109/ACC.2012.6315658.

### *Data Statement*

The datasets generated and analysed during the current study are not available because they require a prior work of processing, formatting and description of their metadata, but the authors will make every reasonable effort to publish them in near future.